Detection of Hypertension Through Features from Heart Rate Variability and Machine Learning Analysis

Aikaterini Vraka[1], Lorenzo Fácila[2], Fernando Hornero[3], Arturo Martínez-Rodrigo[4], Raúl Alcaraz[4], José J Rieta[1]

[1] BioMIT.org, Electronic Engineering Department, Universitat Politecnica de Valencia, Spain
[2] Cardiology Department, General University Hospital Consortium of Valencia, Valencia, Spain
[3] Cardiovascular Surgery Department, Hospital Clínico Universitario de Valencia, Spain
[4] Research Group in Electronic, Biomed. and Telecomm. Eng., Univ. of Castilla-La Mancha, Spain

Abstract

Despite the strong association between hypertension (HT) and heart-rate variability (HRV), the ability of HRV to detect HT cases under the coexistence of several pathologies remains unknown. The present study aims to optimize the HT detection using machine- learning (ML) techniques, in 202 5-minute ECG recordings from the MIMIC database. Recordings were classified by blood pressure (BP) into normotensive (NT), prehypertensive (PHT) and hypertensive (HT) with a cut-off BP of $< 120/80$ *mm Hg,* $\leq 139/89$ *mm Hg and* $\geq$ *140/90 mm Hg, respectively. Time-, frequency-domain and Poincaré HRV features were explored. Multi-class (MC), between-class comparison (BC) and 1-vs-all analysis was performed. Single- (SF) and multifeature (MF) classification with* 10*-fold cross-validation and a* 20% *test set was also performed. Statistically significant differences (*$p \leq 0.022$*) were found in MC and BC for most HRV features. Differences were more prominent in HT group (*$p \leq 0.0003$*). The best MF accuracy for MC was* 95% *using 6 features. HT and NT detection accuracy was* 87.5% *and* 95%*, using 6 and 4 features, respectively, for 1-vs-all analysis. The proposed models can be easily implemented and achieve high classification accuracy. The results suggest the use of HRV to detect HT or HT-prone patients in diseased population.*

1. Introduction

Hypertension (HT) is a widespread disease [1]. Due to the strong association with major health issues, the early HT diagnosis and consistent follow-up are crucial not only in preventing HT but also in reducing mortality risk [1, 2]. HT is defined as blood pressure (BP) $\geq$ 140 mmHg and 90 mmHg for systolic (SBP) and diastolic (DBP) measurements, respectively [1]. So far, the golden standard of HT detection is cuff-based measurements performed with a sphygmomanometer at a doctor's office [1, 3]. Unfortunately, BP measurements are limited to sporadic visits to the doctor or even regular but not continuous home measurements, leaving a possibility of undetected HT events.

Due to this fact, many studies have focused on developing either hardware or software technology that allows the non-stop BP measurement, hence facilitating the HT detection. Hardware-oriented solutions include stress-free cuff-based wearable devices prioritizing comfort and low-volume or cuffless devices functioning in acoustic, tonometry or optical modalities [4, 5]. Even though with lower impact, downsized cuff-based devices are still perceivable. As for cuffless technology, cuff-based calibration or multiple signals are often required [4, 5].

Electrocardiography (ECG) and photoplethysmography (PPG) analysis are two of the most popular software-based solutions for HT detection [6–9]. Both are acquired from routine devices originally used for other health-related measurements, ECG and PPG oriented research has made great steps towards continuous BP monitoring and HT detection. Normally combined together, ECG-PPG analysis allows the estimation of BP by measuring the distance between two fiducial points of the two signals [6, 9]. Besides the fact that this technique is mostly adequate for SBP but not for DBP calculation, the biggest drawback of this method is the requirement of at least two signal sources, which are not always available.

PPG technology is generally more adequate for BP estimation, since PPG signal is a function of the blood volume running through the vessels [6]. Notwithstanding, PPG recordings are extremely sensitive to motion artifacts, which are present in long recordings [9]. On the other hand, ECG alone does not contain direct BP-related information [7]. Even though it is easier to further process the ECGs so that BP-related information is acquired than to efficiently cancel motion artifacts, most studies insist on analyzing PPG for BP-related purposes.

The present study aims to take advantage of the strong association between HT and heart-rate variability (HRV), derived from ECGs, in order to create implementable models that will allow the efficient HT detection. HRV is a measure of the autonomous nervous system calibration, which is strongly associated with BP [10, 11]. Although the HRV-BP interconnection is widely known, only a few HRV-based methods exist to detect HT [12–14]. These studies suffer from gaps in group separation or the inclusion of additional pathologies, deviating the focus from HT detection and putting it to a simple group classification, which does not solve the HT detection problem.

2. Materials and Methods

The database consisted of 202 five-minute ECG recordings of critically-ill people from the MIMIC database [15]. Signals were extracted with a sampling rate of 125 Hz and were resampled to 500 Hz to achieve better resolution. Lead II was analyzed as it was the most frequently available channel. The corresponding arterial BP (ABP) signals were also acquired for classification purposes.

Preprocessing of ECG signals included denoising (powerline interference, muscle noise, baseline wander), ectopics correction and R-peak detection [16–18]. Afterwards, each signal was classified into normotensive (NT), prehypertensive (PHT) and HT with the cut-off being $<$120 mmHg and $\geq$ 140 mmHg for the NT and HT cases, respectively. For this purpose, ABP signals were recruited.

For each recording, time-, frequency-domain and nonlinear HRV features were calculated. Each feature reveals information regarding sympathetic, parasympathetic nervous system or sympathovagal balance. Time-domain features included SDNN, VARNN, RMSSD and pNN50, as described elsewhere, with NN being the interval between successive R peaks after ectopics correction [10,11]. Frequency-domain features included the power at different frequency band as follows: VLF ($<$0.04 Hz), LF ($\leq$ 0.15 Hz), HF ($>$0.15 Hz) and LF/HF [10, 11]. Nonlinear analysis consisted of Poincare indices such as SD1 and SD2, measuring the instantaneous (short-time) and longitudinal (long-time) HRV, respectively [11].

The analysis was performed by comparing/classifying among the three BP groups and by performing an one-vs-all analysis [NT vs PHT & HT (NT/non-NT), NT & PHT vs HT (HT/non-HT)]. Being an intermediate group, one-vs-all analysis with PHT forming a unique category is of no meaning. Comparison was performed with Kruskal-Wallis (KW, three groups) and Mann-Whitney U-test (MWU, one-vs-all). For the classification, the Ensemble method was chosen and the dataset was split with a $80 - 20$ [%] proportion. In order to account for different group size, 10-fold cross validation was performed. For multi-feature classification, values were normalized according to z-score and feature selection was performed after ranking according to ANOVA, considering the combinations that provide the highest test accuracy.

3. Results

Table 1 shows the comparison among the three BP classes (KW test) as well as the comparison in pairs of two and the one-vs-all analysis. For the three-group comparison, statistically significant differences are observed for all features but LF/HF and SD1/SD2, when the PHT and HT classes are compared. As for the comparison between NT and PHT classes, statistically significant differences are only seen for RMSSD, HF and SD1, due to Bonfer-

Table 1. Statistical comparison (p values) between different groups. KW (intergroup) and MWU (in pairs). One vs all: MWU for each pair (NT/non-NT, HT/non-HT). St. sign. diff.: $p \leq 0.05$ for KW and one vs all, $p \leq 0.017$ for the rest.

		NT vs PHT vs HT			One vs all	
Features	**KW**	**NT-PHT**	**PHT-HT**	**NT-HT**	**NT/non-NT**	**HT/non-HT**
mean	< 0.0001	0.8199	0.0001	0.0003	0.0212	< 0.0001
median	< 0.0001	0.8103	0.0001	0.0003	0.0220	< 0.0001
SDNN	< 0.0001	0.9607	< 0.0001	< 0.0001	0.0001	< 0.0001
VARNN	< 0.0001	0.9607	< 0.0001	< 0.0001	0.0001	< 0.0001
RMSSD	< 0.0001	< 0.0001	< 0.0001	< 0.0001	< 0.0001	< 0.0001
pNN50	< 0.0001	0.0348	< 0.0001	< 0.0001	< 0.0001	< 0.0001
VLF	< 0.0001	0.3528	< 0.0001	< 0.0001	0.0062	0.0155
LF	< 0.0001	0.0930	< 0.0001	< 0.0001	< 0.0001	< 0.0001
HF	< 0.0001	< 0.0001	< 0.0001	< 0.0001	< 0.0001	< 0.0001
LF/HF	0.1931	0.0435	0.7370	0.2165	0.0824	0.6115
SD1	< 0.0001	< 0.0001	< 0.0001	< 0.0001	< 0.0001	< 0.0001
SD2	< 0.0001	0.7866	< 0.0001	< 0.0001	0.0007	< 0.0001
SD1/SD2	0.1424	0.0954	0.9709	0.0682	0.0485	< 0.0001

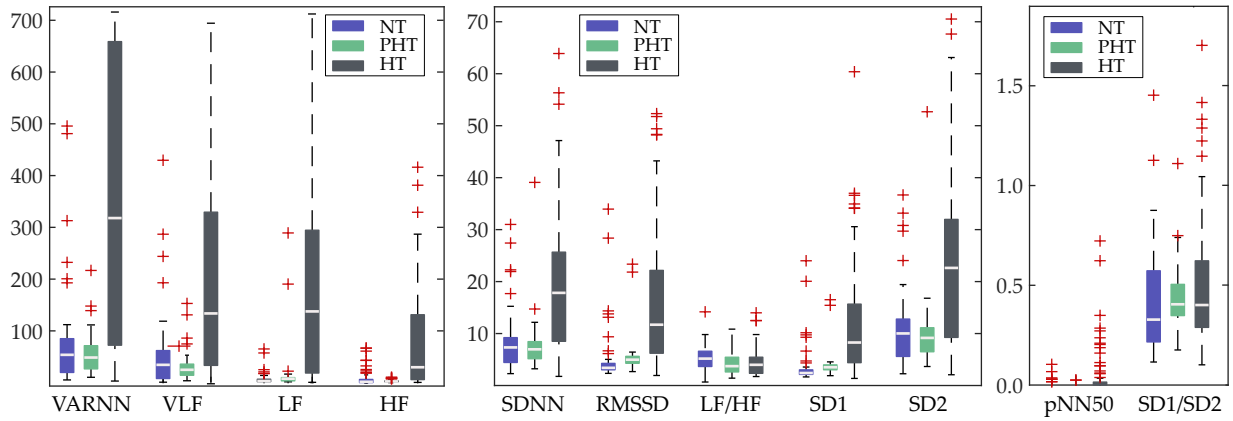

Figure 1. Box and whisker plot for each feature and class. We observe an increment in HT class in most of the features.

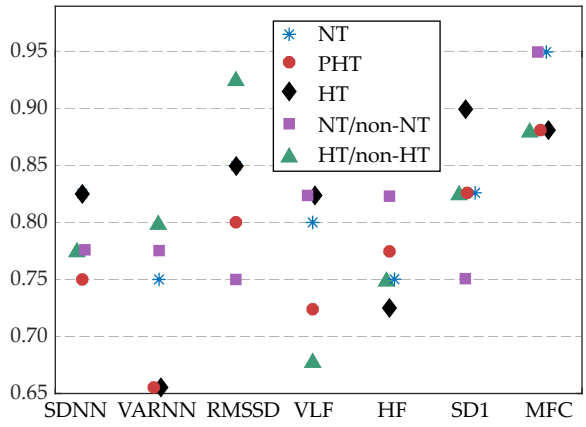

Figure 2. Classification accuracy for the best performing features and the multi-feature classification (MFC).

roni correction. The one-vs-all analysis showed statistically significant differences both when NT and when HT are considered a unique class, suggesting that focusing on the healthy (NT) or the high-risk (HT) group is feasible.

The box and whisker plots of each feature for the three BP classes are illustrated in Figure 1. HRV is remarkably higher in the HT group for most of the features. Additionally considering Table 1, these differences are mostly statistically significant. The only exceptions are LF/HF and SD1/SD2, where values in PHT and HT are comparable, an observation also confirmed by the fact that LF/HF is the only feature that did not show statistically significant difference between the HT and non-HT classes.

The results of the classification among and between classes can be seen in Figure 2, where due to space limits only the accuracy of the best performing single-feature classification problems as well as the accuracy of the multi-feature classification are shown. For the three-class problem, the accuracy is shown considering one time each class as the positive one (NT, PHT, HT). The highest accuracy was observed with multi-feature models. These models consisted of 6 features for the three classes and the HT/non-HT and 4 features for the NT/non-NT. More specifically, for the three-class problem, the median, SDNN, VARNN, RMSSD, pNN50 and VLF were used. For the NT/non-NT classification, VARNN, LF, HF and SD1 were used, while the best results were found using SDNN, VARNN, pNN50, LF, HF and SD1 for the HT/non-HT classification. As it can be seen, most of the features contributing to the multi-feature classification analysis showed themselves quite high classification accuracy.

4. Discussion

The current work suggests the use of HRV-based models to detect HT via ECG signal analysis, which is less prone to motion artifacts compared to PPG. Despite the fact that ECG signals do not contain direct information about BP, HRV, easy to be calculated, is widely connected to BP [11]. For this purpose various time-,frequency-domain and Poincare HRV indices were calculated. The rationale behind the analysis is to study whether HRV is a reliable marker of HT or elevated blood pressure and whether HRV-based models are successful in detecting HT. In order to achieve this, the discriminatory power of HRV features was assesed both by comparing among the three BP classes and by focusing on HT detection (HT/non-HT) and elevated blood pressure detection as the group containing PHT and HT recordings (NT/non-NT). In all cases, statistically significant discrepancies were found.

Afterwards, single- and multi-feature classification analysis was performed, also comparing among and between grouped classes. All in all, the classification accuracy oscillated between 87.5% and 95%, with the detection of elevated BP (NT/non-NT) showing the highest accuracy of 95%, using only 4 features. This result suggests the possibility of computationally simple yet reliable

models that can be implemented in routine ECG devices. This could facilitate the HT detection or the detection of alarming situations in patients with elevated BP. To our knowledge, this is the first study taking advantage of HRV-based features and attempting classification by successive BP classes showing an accuracy as high as 95%.

5. Conclusions

ECG analysis is a high-potential alternative to multi-source signal techniques for HT detection. By taking advantage of the HRV-BP association, simple models can be derived and implemented in monitoring devices, facilitating the HT detection and hindering the development of BP-related health issues.

Acknowledgments

Funding grants PID2021-00X128525-IV0 and PID2021-123804OB-I00 from Spanish Government and European Regional Development Fund (10.13039/501100011033), SBPLY/17/180501/000411 from Junta de Castilla-La Mancha and AICO/2021/286 from Generalitat Valenciana.

References

[1] Visseren FLJ, Mach F, Smulders YM, Carballo D, et al. 2021 ESC guidelines on cardiovascular disease prevention in clinical practice. European heart journal September 2021;42:3227–3337. ISSN 1522-9645.

[2] Lee JY, Bak JK, Kim M, et al. Long-term cardiovascular events in hypertensive patients: full report of the korean hypertension cohort. The Korean journal of internal medicine January 2023;38:56–67. ISSN 2005-6648.

[3] Picone DS, Schultz MG, Armstrong MK, Black JA, et al. Identifying isolated systolic hypertension from upper-arm cuff blood pressure compared with invasive measurements. Hypertension Dallas Tex 1979 February 2021;77:632–639. ISSN 1524-4563.

[4] Altintas E, Takoh K, Ohno Y, Abe K, Akagawa T, et al. Wearable and low-stress ambulatory blood pressure monitoring technology for hypertension diagnosis. Annual International Conference of the IEEE Engineering in Medicine and Biology Society IEEE Engineering in Medicine and Biology Society Annual International Conference 2015; 2015:4962–4965. ISSN 2694-0604.

[5] Kireev D, Sel K, Ibrahim B, Kumar N, et al. Continuous cuffless monitoring of arterial blood pressure via graphene bioimpedance tattoos. Nature nanotechnology August 2022;17:864–870. ISSN 1748-3395.

[6] Allen J. Photoplethysmography and its application in clinical physiological measurement. Physiological measurement March 2007;28:R1–39. ISSN 0967-3334.

[7] Bird K, Chan G, Lu H, Greeff H, Allen J, et al. Assessment of hypertension using clinical electrocardiogram features: A first-ever review. Frontiers in medicine 2020;7:583331. ISSN 2296-858X.

[8] Sun Y, Thakor N. Photoplethysmography revisited: From contact to noncontact, from point to imaging. IEEE transactions on bio medical engineering March 2016;63:463–477. ISSN 1558-2531.

[9] Zhou ZB, Cui TR, Li D, Jian JM, et al. Wearable continuous blood pressure monitoring devices based on pulse wave transit time and pulse arrival time: A review. Materials 2023;16:2133. ISSN 1996-1944.

[10] Heart rate variability. standards of measurement, physiological interpretation, and clinical use. task force of the european society of cardiology and the north american society of pacing and electrophysiology. European heart journal March 1996;17:354–381. ISSN 0195-668X.

[11] Yugar LBT, Yugar-Toledo JC, Dinamarco N, Sedenho-Prado LG, et al. The role of heart rate variability (HRV) in different hypertensive syndromes. Diagnostics Basel Switzerland February 2023;13. ISSN 2075-4418.

[12] Poddar MG, Birajdar AC, Virmani J, Kriti. Automated classification of hypertension and coronary artery disease patients by pnn, knn, and svm classifiers using hrv analysis. Machine Learning in Bio Signal Analysis and Diagnostic Imaging 2019;99–125.

[13] Zhang R, Hua Z, Chen C, Liu G, Wen W. Analysis of autonomic nervous pattern in hypertension based on short-term heart rate variability. Biomedizinische Technik Biomedical engineering August 2020;ISSN 1862-278X.

[14] Ni H, Li Z, Shao Z, Guo M, Liu J. Recoghypertension: early recognition of hypertension based on heart rate variability. Journal of Ambient Intelligence and Humanized Computing 2022;13:3945–3962. ISSN 1868-5137.

[15] Goldberger AL, Amaral LA, Glass L, Hausdorff JM, Ivanov PC, Mark RG, Mietus JE, Moody GB, Peng CK, Stanley HE. Physiobank, physiotoolkit, and physionet: components of a new research resource for complex physiologic signals. Circulation June 2000;101:E215–E220. ISSN 1524-4539.

[16] García M, Martínez-Iniesta M, Ródenas J, Rieta JJ, Alcaraz R. A novel wavelet-based filtering strategy to remove powerline interference from electrocardiograms with atrial fibrillation. Physiological measurement November 2018; 39:115006. ISSN 1361-6579.

[17] Sörnmo L, Laguna P. Electrocardiogram (ECG) Signal Processing, volume 2. United States: John Wiley and Sons. ISBN 978-0-471-24967-2 (set), 2006; 1298–1313.

[18] Martinez A, Alcaraz R, Rieta JJ. A new method for automatic delineation of ECG fiducial points based on the phasor transform. Annual International Conference of the IEEE Engineering in Medicine and Biology Society 2010; 2010:4586–4589. ISSN 2375-7477.

Address for correspondence:

José J. Rieta

BioMIT.org, Electronic Engineering Department, Building 7F, Universitat Politecnica de Valencia, 46022 Valencia, Spain.

e-mail: jjrieta@upv.es